Contribution from Exxon Research and Engineering Company, Annandale, New Jersey 08801

Redox Intercalation Reactions of $VOPO_4 \cdot 2H_2O$ with Mono- and Divalent Cations

A. J. JACOBSON,* JACK W. JOHNSON,* J. F. BRODY, J. C. SCANLON, and J. T. LEWANDOWSKI

Received September 12, 1984

The layered oxide hydrate $VOPO_4 \cdot 2H_2O$ readily undergoes redox intercalation reactions with alkali-, alkaline-earth-, and transition-metal cations in the presence of a reducing agent to form compounds of general composition $M_xVOPO_4 \cdot nH_2O$, where M is the cation and $x \leq 1$. The phase relations as x is varied are complex and have been investigated in detail for sodium and cesium cations by powder X-ray diffraction and chemical analysis. A survey of reactions for the cations Li^+, K^+, Rb^+, Mg^{2+}, Mn^{2+}, Co^{2+}, Ni^{2+}, and Zn^{2+} is described. The interlayer separation of $VOPO_4 \cdot 2H_2O$ contracts upon intercalation of cations with the spacing dependent on specific cation and degree of reduction, while the in-plane tetragonal a axis increases with degree of vanadium reduction, independent of the specific interlayer cation. The intercalation reactions of $VOPO_4 \cdot 2H_2O$ probably proceed via intercalation of the reducing agent and reduction of electronically isolated vanadium(V) sites, in contrast to the redox chemistry of the transition-metal oxides and sulfides, which involves electron transport through the host lattice.

Introduction

Reversible topotactic redox reactions that lead to the formation of solvated intercalation compounds are well-known for the layered transition-metal oxides and dichalcogenides.[1] The general redox intercalation reaction can be written

$$xG^+ + xe^- + y(\text{solv}) + H \rightarrow G^+_x(\text{solv})_yH^{x-}$$

where G and H are general guest species and host lattices, respectively. The guest species G may be a simple or complex metal cation or an organic cation and the solvent is a polar molecule (e.g., H_2O, NH_3, or RNH_2); in some cases the cationic species is the protonated solvent. The reduction of the host lattice H may be carried out by electrochemical means, providing it has reasonable conductivity, or by means of chemical reducing agents. The extent of reduction is determined by the redox properties of the host lattice relative to the solvent system and reducing agent, and also by packing considerations for the guest species in the interlayer space. The interlayer ions and solvent molecules in solvated intercalation compounds have high mobilities and readily undergo ion- and solvent-exchange reactions.

In a previous paper,[2] we described some aspects of the coordination intercalation reactions of the layered mixed oxide hydrates $VOPO_4 \cdot 2H_2O$ and $VOAsO_4 \cdot 2H_2O$ with neutral bases such as pyridine. It was noted that the reaction of $VOPO_4$ with pyridine under some conditions gave dark green products in which a significant fraction of the vanadium(V) had been reduced to vanadium(IV). The products contained both pyridine and pyridinium cations and were shown to be solvated redox intercalation compounds similar to those formed by TaS_2 and MoO_3.[1] This observation led us to examine in more detail the redox intercalation reactions of $VOPO_4 \cdot 2H_2O$. A preliminary account of this work has been reported.[3] It was found that aqueous iodide solutions were convenient reducing agents and that intercalation compounds are formed for most mono- and divalent cations. The general reaction is illustrated by

$$VOPO_4 \cdot 2H_2O + x\text{NaI} \xrightarrow{H_2O} Na_xVOPO_4 \cdot 2H_2O + (x/2)I_2$$

The reaction is rapid at room temperature. The solution phase immediately turns brown as iodide is oxidized to iodine (I_3^- in the presence of excess iodide), and the yellow solid $VOPO_4 \cdot 2H_2O$ turns green as vanadium(V) is partially reduced to V(IV). The layer structure is preserved during the reaction.

Two other brief reports of redox reactions of vanadium phosphate have recently appeared. Hydrogen compounds were prepared by reaction with aqueous hydrazine hydrochloride,[4] and a sodium phase was synthesized by using SO_2 as the reductant.[5] The existence of this class of compounds has also been suggested in earlier papers.[6-8]

In this paper, we describe an extension of our previous work to more detailed characterization of the intercalation compounds of $VOPO_4 \cdot 2H_2O$ particularly with respect to stoichiometry and structure. The synthesis and structural properties of the host lattice were described in a previous paper[2] and are only briefly reviewed here. The structure of $VOPO_4 \cdot 2H_2O$ was first described by Ladwig[9] as a layer lattice built up of neutral $VOPO_4$ layers and interlayer water molecules. More details have subsequently been determined in a single-crystal X-ray study[10] and by powder neutron diffraction.[11] The structure is tetragonal with $a = 6.215$, $c = 7.403$ Å (Figure 1). The vanadium atom lies on a fourfold axis and is surrounded by six oxygen atoms to give a distorted octahedron. The four equatorial oxygens are provided by four different phosphate tetrahedra. One of the axial vanadium–oxygen bond distances is very short (1.567 Å), corresponding to a vanadyl group, V=O. The other axial vanadium–oxygen distance involving the coordinated water molecule is long (2.233 Å). Each VO_6 octahedron is linked to four phosphate tetrahedra, and each tetrahedron, to four octahedra to make up the layers. The second water molecule is inserted between two phosphate tetrahedra in adjacent layers. While the general features of the structure are undoubtedly correct, there are significant differences in the details as determined by the two studies. Some of the differences probably arise from the insensitivity of the neutron experiment to the vanadium atom position. The structure of the analogous $VOAsO_4 \cdot 2H_2O$ has not been determined. However, the similarity of its powder pattern to that of the phosphate and its dehydration behavior strongly suggest that the arsenate and phosphate are isostructural.[12] The lattice parameters reported for the arsenate are $a = 6.37$, $c = 7.39$ Å.

Experimental Section

Powder X-ray diffraction patterns were obtained with either a Philips wide-angle goniometer or an automated Siemens D500 diffractometer using graphite-monochromated Cu Kα radiation. Samples were equilibrated at 54% RH before measurements were made. Infrared spectra were measured in KBr disks with a Digilab Fourier transform instrument. Thermogravimetric analyses were carried out on a Du Pont Model 1090 thermal analyzer at a heating rate of 10 °C/min from room temperature

(1) Schöllhorn, R. In "Intercalation Chemistry"; Whittingham, M. S., Jacobson, A. J., Eds.; Academic Press: New York, 1982; pp 315-360.
(2) Johnson, J. W.; Jacobson, A. J.; Brody, J. F.; Rich, S. M. *Inorg. Chem.* **1982**, *21*, 3820-3825.
(3) Johnson, J. W.; Jacobson, A. J. *Angew. Chem., Int. Ed. Engl.* **1983**, *22*, 412-413; *Angew. Chem.* **1983**, *95*, 422.
(4) Zazhigalov, V. A.; Pyatnitskaya, A. I.; Bacherikova, I. V.; Komashko, G. A.; Ladwig, G.; Belousov, V. M. *React. Kinet. Catal. Lett.* **1983**, *23*, 119-123.
(5) Casañ-Pastor, N.; Beltrán-Porter, D.; Martinez-Tamayo, E. *Neuvieme Journée d'Etude des Equilibres entres Phases* 1983, 77-80.
(6) Thilo, E.; Ladwig, G. *Omagiu Raluca Ripan* **1966**, 607-612.
(7) Seeboth, H.; Kubias, B.; Wolf, H.; Lücke, B. *Chem. Tech. (Leipzig)* **1976**, *28*, 730-734.
(8) Seeboth, H.; Ladwig, G.; Kubias, B.; Wolf, G.; Lücke, B. *Ukr. Khim. Zh.* **1977**, *43*, 842-844.
(9) Ladwig, G. *Z. Anorg. Allg. Chem.* **1965**, *338*, 266-278.
(10) Tietze, H. R. *Aust. J. Chem.* **1981**, *34*, 2035-2038.
(11) Tachez, M.; Theobald, F.; Bernard, J.; Hewat, A. W. *Rev. Chim. Miner.* **1982**, *19*, 291-300.
(12) Chernorukov, N. G.; Egorov, N. P.; Korshunov, I. A. *Zh. Neorg. Khim.* **1978**, *23*, 2673-2675; *Russ. J. Inorg. Chem. (Engl. Transl.)* **1978**, *23*, 1479-1481.

0020-1669/85/1324-1782$01.50/0

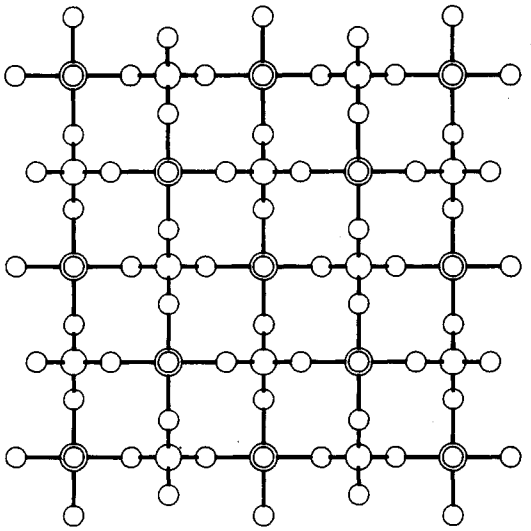

Figure 1. Layer structure of $VOPO_4 \cdot 2H_2O$ viewed down the c axis.

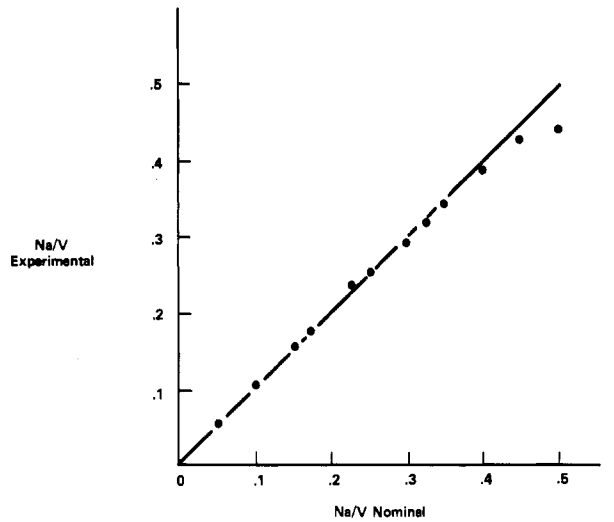

Figure 2. Experimental vs. nominal compositions for $Na_xVOPO_4 \cdot 2H_2O$.

to 600 °C. Elemental analyses for V, P, and intercalated metals were performed by Galbraith Laboratories, Knoxville, TN. Vanadium oxidation states were determined by a redox titration procedure. Samples were dissolved in dilute sulfuric acid, and then the V(IV) oxidized to V(V) with excess ceric ammonium nitrate. The solution was then back-titrated with Fe(II) solution to reduce first the excess cerium and then the V(V) to V(IV). This procedure gives the amount of V(IV) and the total vanadium present in the sample. The end points were determined potentiometrically by using an Orion platinum redox electrode in conjunction with a Fisher Titrimeter II automatic titrator. The synthesis of the host lattices has been described previously.[2]

Synthesis of Intercalation Compounds. Intercalation compounds, $M_xVOPO_4 \cdot 2H_2O$, were prepared by reaction at ambient temperature of small samples (0.3–0.5 g) of solid $VOPO_4 \cdot 2H_2O$ with stoichiometric amounts of a 0.25–0.5 M solution of the metal iodide in water or 95% ethanol/water in an automatic shaker. For small values of x, excess solvent was added to bring the total volume up to 3 mL. Reaction times of 1–3 days were used. The solid products were filtered, washed with solvent to remove any excess iodine, and air-dried. Upper limits on the value of x in $M_xVOPO_4 \cdot 2H_2O$ were determined by reaction in a fourfold excess of metal iodide solution. The choice of solvent is determined by the solubility of the metal iodide and of the solid host. This general procedure has been used to prepare intercalation compounds of Li^+, Na^+, K^+, Rb^+, Cs^+, Mg^{2+}, Mn^{2+}, Co^{2+}, Ni^{2+}, and Zn^{2+}.

Results

Redox Intercalation of $VOPO_4 \cdot 2H_2O$ with Sodium Iodide. A series of 20 samples was prepared by addition of stoichiometric amounts of a 0.25 M solution of sodium iodide in 95% ethanol to 0.5-g samples of $VOPO_4 \cdot 2H_2O$. The sodium to vanadium ratios for the intercalation compounds were determined by elemental analysis are compared with the nominal compositions in Figure 2. The good agreement observed for Na/V < 0.35 indicates that the reaction is stoichiometric. For Na/V ratios >0.35, the measured values are lower than the nominal compositions, suggesting that the reaction slows down as the limiting composition is approached. The stoichiometry of the reaction was confirmed in two experiments by analysis of both the solution and solid phases after the reaction. The results demonstrated negligible solubility of the intercalation compounds in 95% ethanol/water.

Table I. X-ray Diffraction Data for the $Na_xVOPO_4 \cdot 2H_2O$ Phases

x	a, Å	c,[a] Å	phase
0.057			VP,[b] III, II
0.055			VP, III, II
0.109			VP, III, II
0.120			VP, III, II
0.159	6.218 (4)	13.522 (8)	VP, II[c]
0.170	6.218 (4)	13.501 (6)	III, II[c]
0.179	6.222 (3)	13.494 (6)	VP, II[c]
0.200	6.221 (4)	13.457 (9)	II
0.240	6.226 (2)	13.431 (4)	II
0.258	6.226 (3)	13.398 (6)	II
0.26	6.236 (4)	13.391 (5)	II
0.275	6.228 (2)	13.399 (4)	II
0.294	6.231 (2)	13.362 (5)	II
0.30	6.236 (2)	13.351 (5)	II
0.320	6.237 (2)	13.349 (4)	II
0.345	6.232 (3)	13.310 (5)	II,[c] I
0.388		13.04	II, I[c]
0.430	6.270 (2)	13.053 (5)	II, I[c]
0.441	6.262 (4)	13.037 (8)	II, I[c]
0.460	6.260 (2)	13.044 (5)	II, I[c]

[a] Interlayer separation for all $Na_xVOPO_4 \cdot 2H_2O$ phases is $c/2$. [b] $VOPO_4 \cdot 2H_2O$. [c] Phase for which lattice parameters determined.

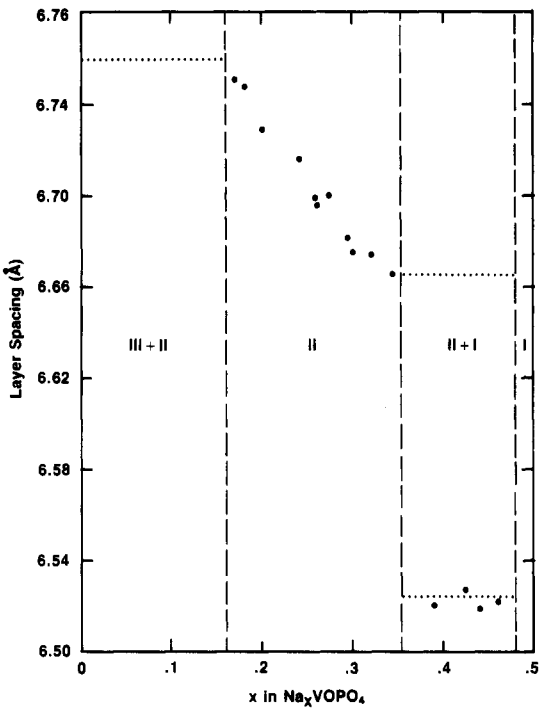

Figure 3. Layer spacing vs. x in $Na_xVOPO_4 \cdot 2H_2O$ showing the regions of single-phase and two-phase behavior. Points (●) are values for least-squares-refined layer spacings.

The lattice parameters of the sodium intercalation compounds were determined by least-squares fitting the data in the range $10° < 2\theta < 60°$. The results are summarized in Table I and Figure 3. Three distinct phases are observed in the $Na_xVOPO_4 \cdot 2H_2O$ system: a phase with low but unknown sodium content (phase III), a nonstoichiometric region with $0.16 < x < 0.33$ (phase II), and a nearly stoichiometric phase with $x = 0.48$–0.50 (phase I). Phase I and phase II samples were shown by thermogravimetric analysis to contain 2 H_2O/vanadium. Data for $VOPO_4 \cdot 2H_2O$ (weight loss 18.3% obsd, 18.2% calcd), $Na_{0.46}VOPO_4 \cdot 2H_2O$ (phase I, 17.0% obsd, 17.3% calcd), and $Na_{0.25}VOPO_4 \cdot 2H_2O$ (phase II,

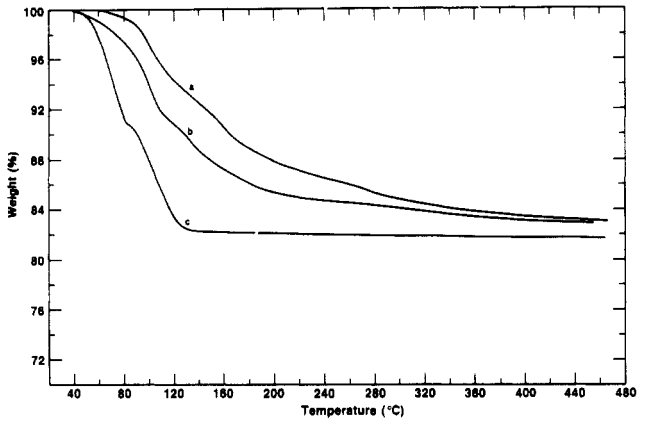

Figure 4. Thermogravimetric analysis data for (a) $Na_{0.46}VOPO_4 \cdot 2H_2O$, (b) $Na_{0.245}VOPO_4 \cdot 2H_2O$, and (c) $VOPO_4 \cdot 2H_2O$ at 10 °C/min in oxygen.

17.2% obsd, 17.6% calcd) are shown in Figure 4. Pure $VOPO_4 \cdot 2H_2O$ loses two water molecules in two well-resolved steps. Intercalation of sodium cations increases the dehydration temperature and blurs the distinction between the two kinds of water molecule.

The results used to establish the phase relations shown in Figure 3 are discussed in more detail below for three different composition ranges.

Range 1: $x < 0.20$. Three phases are observed when $x < 0.20$: unreacted $VOPO_4 \cdot 2H_2O$ (c = 7.40 Å) and intercalation compounds with c = 7.13 Å (phase III) and c = 6.75 Å (phase II). For compositions with $x < 0.16$, all three phases are observed and the X-ray patterns contain too many overlapping reflections to allow accurate determination of lattice parameters. In the range $0.16 < x < 0.20$ the major phase present is phase II but the samples also contain either phase III or $VOPO_4 \cdot 2H_2O$. Equilibrium is clearly not achieved in this composition range. Attempts to improve the situation by raising the reaction temperature or by equilibration of multiphase samples in electrolyte solutions were not successful.

Range 2: $0.2 < x < 0.32$ (Phase II). All of the samples prepared with $0.2 < x < 0.32$ are single phase II. The major peaks in the X-ray patterns correspond to a tetragonal lattice with an a axis similar to that of $VOPO_4 \cdot 2H_2O$ but with a substantially contracted c axis. However, several weak intensities are also observed that can only be indexed by using a doubled c axis parameter. As the sodium content increases, the c axis spacing decreases (Figure 3) confirming that phase II is a single nonstoichiometric phase with a composition range of at least $0.2 < x < 0.32$. The position of lower phase boundary is difficult to determine because of the equilibration problems discussed above. However, we note that the sample with $x = 0.159$ contained only a very small amount of second phase, suggesting that the lower limit for phase II lies somewhat below $x = 0.20$. The upper phase boundary is discussed below.

Range 3: $0.35 < x < 0.46$. Samples with $0.35 < x < 0.46$ are all two-phase mixtures of phase II and phase I. Phase I has an even smaller c axis parameter than phase II, as can be seen in the comparison of the X-ray patterns shown in Figure 5. The relative amounts of the two phases present, estimated from the diffraction data, are as expected for an *equilibrium* mixture of phases I and II. The changes in relative intensities of the (003) reflections with composition were used to obtain the upper composition limit for phase II and the lower limit for phase I. An extrapolation of the data for five compositions gave $x = 0.33$ as an upper limit for phase II and $x = 0.48$ as the lower limit for phase I. Data for samples prepared with excess sodium iodide at ambient temperature suggest an upper limit of $x = 0.5$ for phase I. At higher temperatures (50–75 °C) and with longer reaction times, very disordered compounds with higher sodium contents ($x < 0.68$) were observed.

Single phase I sodium intercalation compounds may also be prepared under similar reaction conditions using excess aqueous

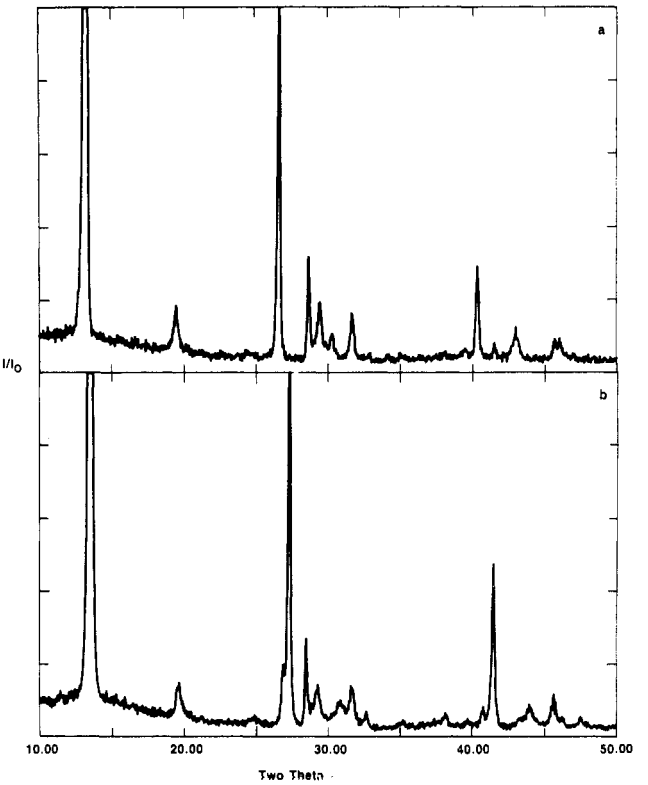

Figure 5. Powder X-ray diffraction patterns for (a) $Na_{0.245}VOPO_4 \cdot 2H_2O$ (phase II) and (b) $Na_{0.46}VOPO_4 \cdot 2H_2O$ (phase I).

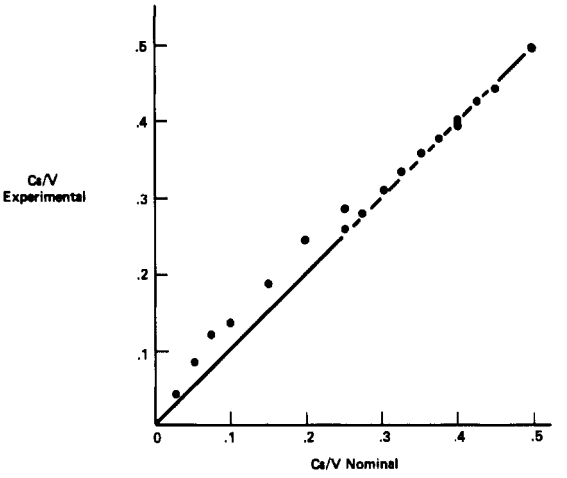

Figure 6. Experimental vs. nominal compositions for $Cs_xVOPO_4 \cdot 1.8H_2O$.

sodium iodide. With substoichiometric amounts of aqueous iodide, the results are identical with those obtained with 95% ethanol/water as the solvent, provided $x > 0.4$. Reactions in aqueous solution with $x < 0.4$ resulted in compounds with compositions that were higher than expected from the nominal stoichiometry, indicating some vanadium(V) host lattice dissolution.

Redox Intercalation of $VOPO_4 \cdot 2H_2O$ with Cesium Iodide. Preliminary reactions were carried out with water as a solvent for the cesium iodide and 2-day reaction times. Eighteen compositions were prepared at ambient temperature. The cesium to vanadium ratios in the intercalation compounds were determined by elemental analysis and are compared with the nominal compositions in Figure 6. The results show that for compositions with $x > 0.275$ the reaction is stoichiometric. The kinetics are slow for compositions with $x > 0.4$, and the point at $x = 0.496$ in Figure 6 corresponds to a reaction time of 4 days. Below $x = 0.275$, the measured compositions are higher than the nominal values, indicating some solid dissolution. However, in view of the generally good agreement, the reactions were not repeated in ethanol.

Table II. Lattice Parameters for Phases I and II of $Cs_xVOPO_4 \cdot 1.8H_2O$

x	a, Å	c,[a] Å	phase
0.133	6.226	13.860	II
0.186	6.223	13.820	II
0.245	6.227 × 2	13.738	II
0.264[b]	6.224	13.700	II
0.309[b]	6.246	13.620	II
0.496	6.268	14.110	I

[a] Interlayer separation for $Cs_xVOPO_4 \cdot 1.8H_2O$ phases is $c/2$. [b] Contains a small amount of phase I.

The intercalation behavior of $VOPO_4 \cdot 2H_2O$ with cesium ions is generally similar to that observed in the sodium system. Two phases are observed: a nonstoichiometric compound with $0.12 < x < 0.30$ (phase II by analogy with the sodium system) and a nearly stoichiometric composition with $x = 0.5$ (phase I). Water contents of both phases were determined thermogravimetrically to correspond to 1.8 $H_2O/VOPO_4$. The discussion of phase behavior observed by X-ray diffraction is conveniently divided into three composition ranges.

Range 1: $x \leq 0.12$. Samples with compositions $x = 0.039$, 0.082, and 0.119 contain a phase with a contracted c axis (phase II) and unreacted $VOPO_4 \cdot 2H_2O$. The amount of unreacted $VOPO_4 \cdot 2H_2O$ decreases as x increases. The mixed reflections for the phase II components in these three samples are poorly defined, but the $00l$ reflections give an average c-axis spacing of 6.930 (5) Å.

Range 2: $0.12 < x < 0.32$. The compounds prepared in this composition range are predominantly single phase II. The X-ray patterns were indexed with tetragonal unit cells (Table II), analogous to the results for the corresponding phase II sodium intercalation compounds. Phase limits were not determined precisely because equilibrium is difficult to achieve near phase boundaries. However, phase II extends approximately from $x = 0.12$ up to $x = 0.30$. In two samples, several weak reflections were observed that could not be accounted for by the $a \times 2c$ unit cell. These reflections were much better developed in a single-phase sample with $x = 0.245$, which was prepared by using 10–50-μ crystallites of $VOPO_4 \cdot 2H_2O$ rather than the usual 2–10-μ size range. The powder pattern of this sample was completely indexed with both doubled a and c axes (see Table II).

Range 3: $0.32 < x < 0.5$. Seven samples prepared in this composition range ($x = 0.332$, 0.360, 0.377, 0.395, 0.400, 0.408, and 0.427) were all two-phase mixtures of phase II and phase I and contained decreasing amounts of phase II with increasing x. A single phase I sample, with $x = 0.496$, was prepared by reaction for 4 rather than 2 days. The phase I components of all of the two-phase mixtures have lattice constants closely similar to those of the single phase with $x = 0.496$, indicating that the lower composition limit of phase I does not extend much below $x = 0.5$.

The interlayer separation of 7.055 Å in phase I is expanded by 0.1–0.2 Å relative to the spacings in phase II, in contrast to the contraction in layer spacing observed for the corresponding sodium phases. The cesium phase I compound also has inverted $00l$ intensities in the X-ray pattern ($I(002) > I(001)$) due to cancellation of X-ray scattering from the layers with the large scattering from the interlayer cesium ions.

Redox Intercalation of $VOPO_4 \cdot 2H_2O$ with the Other Alkali-Metal Iodides. A survey of the redox intercalation reactions of $VOPO_4 \cdot 2H_2O$ with lithium, potassium, and rubidium iodides was carried out for a small number of compositions. The results are summarized in Table III. All three alkali metals gave predominantly single-phase products with compositions close to $x = 0.25$, analogous to phase II observed for both the sodium and cesium intercalation compounds. The lithium results show, in addition, evidence for the formation of a phase I intercalation compound ($x = 0.4$–0.5) and also the formation of a new phase $LiVOPO_4 \cdot 2H_2O$ in which all of the vanadium(V) has been reduced to vanadium(IV). The results for potassium and rubidium at compositions other than at $x = 0.25$ are complex. The potassium compound formed with $x = 0.64$ is apparently single phase but has an unusually low water content. The rubidium data indicate the formation of a compound with $x \sim 1/2$. However, the diffraction data reported in Table III for the rubidium compounds contain a number of intensities that cannot be indexed by the $a \times 2c$ tetragonal cell. The nature of these compositions is consequently uncertain. In particular, a broad diffraction line with $d = 3.85$ Å is observed in all rubidium samples.

Table III. Intercalation Compounds of $VOPO_4 \cdot 2H_2O$ with Lithium, Potassium, and Rubidium: $M_xVOPO_4 \cdot yH_2O$

cation	I^-/V (reactants)	x(product)	a, Å	c,[a] Å	y
lithium	2.0	1.0	6.350	12.811	2.0
	0.75	0.54	6.277	13.211	1.98
	0.5	0.40	6.265	13.223	1.94[b]
			6.22	14.20	
	0.5	0.4	6.265	13.293	2.14
			6.257	13.377	
	0.25	0.23	6.231	14.168	2.33[b]
potassium	2.0	0.64	6.300	12.752	1.51
	0.5	0.45	6.272	12.754	1.46[b]
				13.530	
	0.25	0.246	6.242	13.365	2.05[b]
rubidium	2.0	0.52	6.280	12.943	1.62
	0.5	0.46	6.268	12.963	1.75
	0.25	0.239	6.246	13.407	1.82

[a] Interlayer separation for all $M_xVOPO_4 \cdot yH_2O$ phases is $c/2$. [b] Denotes major phase in two phase products.

Table IV. Intercalation Reactions of $VOPO_4 \cdot 2H_2O$ with Divalent Cations

cation	I^-/V (reactants)	V^{4+}/V^{5+} (product)	phases
magnesium	0.25	0.30	2 phase[a]
	0.50	0.44	single
	2.00	0.92	single[b]
manganese	0.25	0.33	complex multiphase[a]
	0.50	0.45	single
	2.00	0.72	2 phase
cobalt	0.25	0.31	3 phase[a]
	0.50	0.50	single
	2.00	0.76	single
nickel	0.25	0.50	single
	0.50	0.47	single
	2.00	0.73	3 phase[b]
zinc	0.25	0.39	3 phase[a]
	0.50	0.60	single
	2.00	0.86	2 phase[b]

[a] Contains the phase with the next highest composition. [b] Indicates the presence of a higher hydrates.

Redox Intercalation Reactions of $VOPO_4 \cdot 2H_2O$ with Divalent-Metal Iodides. A survey of the phases formed on redox intercalation of $VOPO_4 \cdot 2H_2O$ was carried out for the divalent cations of magnesium, manganese, cobalt, nickel, and zinc by using 0.25, 0.5, and 2.0 equiv of the iodides in aqueous solution. The use of aqueous solutions gave problems with vanadium phosphate solubility, but ethanol could not be used because of low solubility of the divalent iodides. The extent of intercalation and the phase purity of the products are summarized in Table IV. Addition of 0.25 equiv of iodide should lead to the same V(IV) content in the product as found in the phase II alkali-metal phases but with half the concentration of interlayer cations. However, the use of aqueous solutions of the divalent-metal iodides led to solid dissolution and consequent overreduction, the effect being least pronounced for magnesium ($[V^{4+}] = 0.30$) and most for nickel ($[V^{4+}] = 0.50$). Except for the nickel sample, which has a V(IV) content analogous to the alkali-metal phase I, the products are two-phase mixtures. In contrast, the analytical data for the products formed by addition of 0.5 equiv of added iodide show that, except for the case of zinc, the reaction is nearly stoichiometric ($[V^{4+}] = 0.44$–0.54). The intercalation compounds (analogous to phase I but with $x = 1/4$) are single phase by X-ray diffraction but not well ordered. Approximate lattice constants

Table V. Lattice Parameters and Water Contents for the Single-Phase Divalent-Metal Intercalation Compounds $M_xVOPO_4 \cdot yH_2O$

cation	x	a, Å	c, Å	y
Mg[a]	0.22	6.27 (1)	6.62 (1)	3.63
Mg	0.46	6.33 (1)	9.16 (2)	3.58
Mn	0.225		6.48 (2)	2.53
Co	0.25	6.28 (1)	6.59 (1)	2.35
Ni	0.235	6.27 (1)	6.61 (1)	2.31
Zn	0.30	6.28 (1)	6.63 (1)	2.56

[a] X-ray data correspond to a partially dehydrated sample.

are given in Table V determined from the 00*l* and *hk*0 reflections. Evidence for a doubling of the *c* axis is found only for the zinc and magnesium compounds.

Compounds prepared with excess reducing agent showed varying degrees of reduction from a low at Mn ($[V^{4+}] = 0.72$) to a high at Mg ($[V^{4+}] = 0.92$). The X-ray patterns were poorly defined for cations other than magnesium and complicated by the appearance of more highly hydrated phases. The magnesium intercalation compound, stable at ambient humidity, is a single-phase higher hydrate $Mg_{0.46}VOPO_4 \cdot 3.58H_2O$ with $c = 9.16$ Å. When heated to 110 °C, it loses water and $Mg_{0.46}VOPO_4 \cdot 1.93H_2O$ is formed, with a decrease in *c*-axis spacing to 6.62 Å. The single-phase intercalation compound $Mg_{0.22}VOPO_4 \cdot 3.63H_2O$ shows similar behavior, but the extra water molecules are lost at lower temperature.

Discussion

Vanadium phosphate readily undergoes redox intercalation reactions with alkali-metal and alkaline-earth-metal cations in the presence of a reducing agent. While iodide was the reducing agent of choice, $N_2H_4 \cdot 2HCl$, $NH_2OH \cdot HCl$, Fe^{2+}, Sn^{2+}, SO_3^{2-}, and HNO_2 also proved effective. The phase relations are complex, and the reactions are complicated by significant solubility of the host lattice in water. Equilibrium is difficult to achieve at ambient temperature at both low and high levels of reduction. When the concentration of reductant is low, nucleation effects lead to overreduction of some crystallites. At higher levels of reduction, transformation between two intercalated phases appears to be rate limiting. All of the cations studied show complex phase relations for the intercalation compounds, and each system has several phases with different degrees of nonstoichiometry. Only the smallest cations, lithium and magnesium, form intercalation compounds in which all of the vanadium(V) is reduced to vanadium(IV).

The phase relations in redox intercalation reactions are best studied by electrochemical methods. This is precluded for vanadium phosphate by the low electronic conductivity of the host lattice and also of the intercalation compounds themselves. Attempts at electrochemical reduction using cathodes containing large amounts (50 wt %) of graphite to assist current collection were unsuccessful. The lack of electrochemical reactivity raises a question about the mechanism of the reaction, since redox intercalation generally requires both ionic transport of the guest in the interlayer region and electron transport in the host lattice. We propose that in this case the reductant, I^-, is itself intercalated and subsequently expelled in oxidized form. A similar mechanism has recently been proposed for intercalation of α-$RuCl_3$.[13] Electrochemical reduction of this system can occur in an Na^+/H_2O electrolyte solution, with up to 0.5 electron/Ru transferred to the host. At this composition the host lattice becomes insulating and further reduction with up to 1.0 electron/Ru transferred can only be achieved by chemical reaction with sodium dithionite.

Vanadium reduction on intercalation results in an increase in the *a* dimension of the host lattice, which is independent of the specific interlayer cation. A comparison of the equatorial V–O bond lengths in $VOPO_4 \cdot 2H_2O$ with comparable bond lengths in $VOSO_4$ phases gives an estimate of the expansion that might be

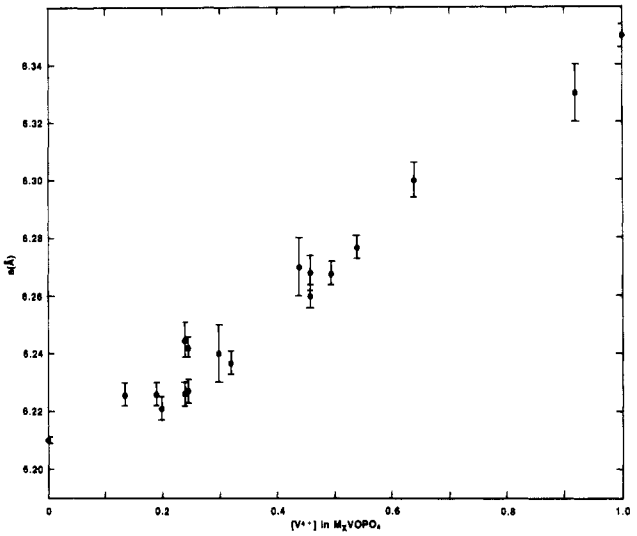

Figure 7. Tetragonal *a* axis vs. mole fraction of V^{4+} in $M_xVOPO_4 \cdot nH_2O$ (M = monovalent or divalent cation).

expected. The mean equatorial V–O bond length in the phases α- and β-$VOSO_4$, $VOSO_4 \cdot 3H_2O$, $VOSO_4 \cdot 5H_2O$, β-$VOSO_4 \cdot 5H_2O$, $VOSO_4 \cdot 3H_2O$, and $VOSO_4 \cdot 0.5H_2SO_4$[14,15] is 2.028 Å. The corresponding distance in $VOPO_4 \cdot 2H_2O$ is 1.908 Å, and consequently a maximum expansion of 0.24 Å (2 × 0.12 Å) in *a* is predicted when $VOPO_4 \cdot 2H_2O$ is reduced to $M^{I}_{1.0}VOPO_4 \cdot 2H_2O$ or $M^{II}_{0.5}VOPO_4 \cdot 2H_2O$. In practice a smaller change will be observed if the octahedra are rotated so that the O–V–O axis is not parallel to *a* and if the O–V–O angle becomes more acute. The measured values for the tetragonal *a* axes for both mono- and divalent cations are plotted against $[V^{4+}]$ in Figure 7. A good correlation is observed. $LiVOPO_4 \cdot 2H_2O$, which contains only V(IV), shows an *a*-axis expansion of 0.135 Å relative to $VOPO_4 \cdot 2H_2O$.

Intercalation of cations into the $VOPO_4 \cdot 2H_2O$ structure causes a reduction of the interlayer separation. In the host lattice the layers are held together by relatively weak hydrogen bonding. On intercalation, the layers become negatively charged and are brought closer together by electrostatic interaction with the interlayer cations. The changes are difficult to interpret quantitatively. The degree of hydration varies with the ratio of the charge to radius of the intercalated cation, but for the large cations, the cation diameter rather than the size of the water molecules determines the interlayer spacing. These two factors can be seen in the data for the alkali-metal intercalation compounds (Figure 8). The results at a composition of $x = 0.25$ show a pronounced minimum in the interlayer separation with increasing cation radius. The lithium compound has the highest degree of hydration; the large *c* axis for cesium arises because of the large cation diameter (3.38 Å) even though the degree of hydration is lowest in the series. The results for the alkali-metal compounds with $x = 0.5$ show similar behavior excluding potassium, which does not form a single phase at this composition. The lithium results show that the *c*-axis spacing progressively decreases as the layer charge is increased.

In the X-ray data of the intercalation compounds where the mixed reflections (h, k, $l \neq 0$) are well defined, a doubling of the *c* axis is required to index the powder patterns. It is not yet known whether the *c*-axis doubling arises from a translation of one layer relative to the next on intercalation or from the occupation of different cation sites in alternate layers. In the structurally related $NH_4SbFPO_4 \cdot H_2O$,[16] a translation along the (110) direction of one layer relative to the next leads to a doubled *c* axis.

The higher charge to radius ratio of the divalent cations results in the formation of higher hydrates, as observed in the di-

(13) Schöllhorn, R.; Steffen, R.; Wagner, K. *Angew. Chem.* **1983**, *95*, 559; *Angew. Chem., Int. Ed. Engl.* **1983**, *22*, 555.

(14) Tachez, M.; Theobald, F. *Acta Crystallogr., Sect. B: Struct. Crystallogr. Cryst. Chem.* **1980**, *B36*, 2873–2880.

(15) Tachez, M.; Theobald, F. *Acta Crystallogr., Sect. B: Struct. Crystallogr. Cryst. Chem.* **1980**, *B37*, 1978–1982.

(16) Mattes, R.; Holz, K. *Angew. Chem., Int. Ed. Engl.* **1983**, *22*, 872–873; *Angew. Chem.* **1983**, *95*, 898.

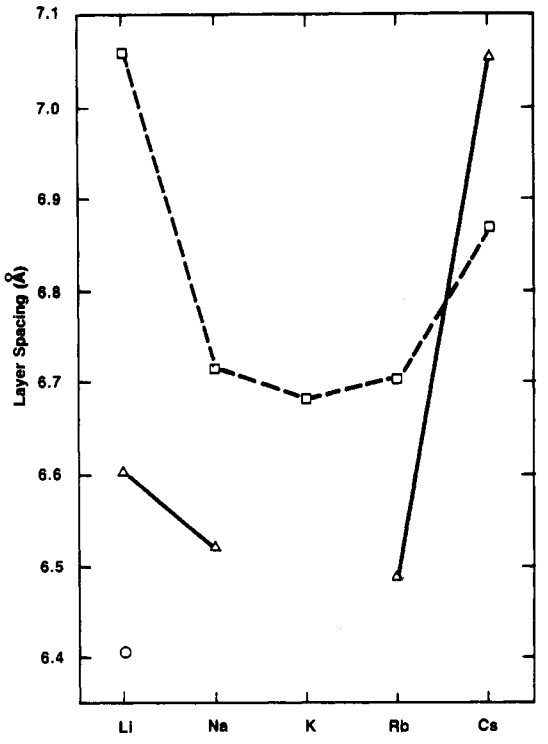

Figure 8. Interlayer separation for the alkali-metal-intercalation compounds at $x = 0.25$ (■), $x = 0.5$ (△), and $x = 1$ (○).

chalcogenides. For example, the intercalation compound $Mg_{0.46}VOPO_4 \cdot 3.58H_2O$ is stable at ambient humidity. The interlayer spacing of this phase (9.16 Å) is larger than that for the corresponding lithium compound at the same level of reduction (6.405 Å). The unit cell volumes of $LiVOPO_4 \cdot 2H_2O$ and $Mg_{0.46}VOPO_4 \cdot 3.58H_2O$ are 258.3 and 367.03 Å^3, respectively. The increase in volume of 108.7 Å^3 corresponds to the intercalation of 2×1.58 H_2O molecules/unit cell ($Z = 2$). The volume per water molecule is thus calculated to be 34.4 Å^3, in good agreement with values measured for water in zeolites (~33 Å^3) or the value for liquid water (30 Å^3).

Finally, we note that intercalation reactions can be carried out under the same general conditions for the isostructural host lattice $VOAsO_4 \cdot 2H_2O$. Problems associated with host lattice solubility are substantially worse for the arsenate than for the phosphate. However, infrared data for the sodium and lithium intercalation compounds of $VOAsO_4 \cdot 2H_2O$ clarify an important point. In vanadium phosphate and its intercalation compounds, the characteristic V=O stretching frequency at about 1000 cm^{-1} is masked by PO_4 vibrations. In the arsenic analogue, the arsenate bands are at significantly lower energy and the vanadyl stretching mode at 1010 cm^{-1} is clearly distinguished in $VOAsO_4 \cdot 2H_2O$ (Figure 9). On intercalation by lithium or sodium to give a compound of stoichiometry $M_{0.5}VOAsO_4 \cdot 2H_2O$ the V=O band splits (e.g., for Na in Figure 9) to give two bands, one characteristic of V^V=O at 1013–1015 cm^{-1} and one from V^{IV}=O at 992 cm^{-1}. Complete reduction to V(IV) in $LiVOPO_4 \cdot 2H_2O$ results again in a single V=O stretching frequency at 1020 cm^{-1} (Figure 10). The infrared data support the model of strong localization of the transferred charges at the vanadium sites in the structure.

In conclusion, we have shown that $VOPO_4 \cdot 2H_2O$ and $VOAsO_4 \cdot 2H_2O$ are versatile hosts for intercalation chemistry. In addition to the coordination intercalation reactions described previously,[2] these compounds will intercalate a wide variety of cations when treated with suitable reducing agents. The detailed phase behavior of the resulting intercalation compounds can be quite complex. The difficulty in studying the phase relationships highlights the unique aspect of these intercalation compounds. The host lattices are not good electronic conductors, even after intercalation. Consequently, the intercalation reactions of vanadium phosphate probably proceed via intercalation of the reducing agent, in contrast to the well-studied redox intercalation of the transition-metal oxides and sulfides that involve electron transport through the host lattice.

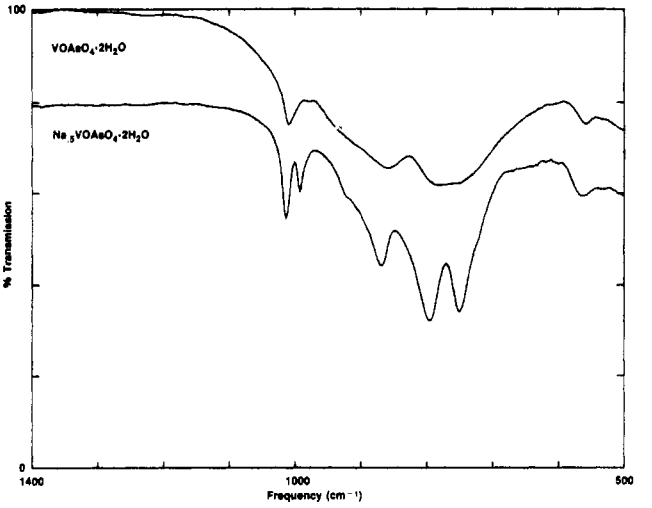

Figure 9. Infrared data for $VOAsO_4 \cdot 2H_2O$ and $Na_{0.5}VOAsO_4 \cdot 2H_2O$.

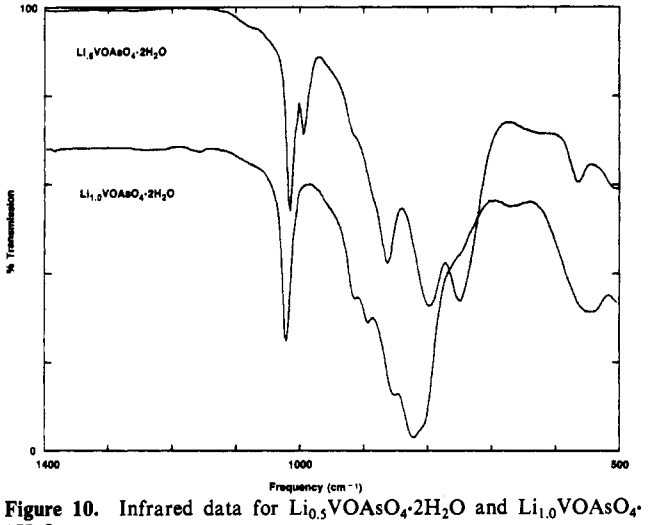

Figure 10. Infrared data for $Li_{0.5}VOAsO_4 \cdot 2H_2O$ and $Li_{1.0}VOAsO_4 \cdot 2H_2O$.

Acknowledgment. We thank J. M. Newsam for Figure 1.

Registry No. $VOPO_4 \cdot 2H_2O$, 12293-87-7; LiI, 10377-51-2; NaI, 7681-82-5; KI, 7681-11-0; RbI, 7790-29-6; CsI, 7789-17-5; MgI_2, 10377-58-9; MnI_2, 7790-33-2; CoI_2, 15238-00-3; NiI_2, 13462-90-3; ZnI_2, 10139-47-6; Li_xVOPO_4, 96150-46-8; Na_xVOPO_4, 96150-53-7; K_xVOPO_4, 96150-50-4; Rb_xVOPO_4, 96150-51-5; Cs_xVOPO_4, 96150-43-5; Mg_xVOPO_4, 96150-47-9; Mn_xVOPO_4, 96150-48-0; Co_xVOPO_4, 96150-44-6; Ni_xVOPO_4, 96150-49-1; Zn_xVOPO_4, 96150-54-8; $LiVOPO_4 \cdot 2H_2O$, 96130-52-8; $VOAsO_4 \cdot 2H_2O$, 12291-57-5; Na_xVOAsO_4, 96150-52-6; Li_xVOAsO_4, 96150-45-7; $LiVOAsO_4$, 96130-51-7.